Isotopic Equivalence by Bézier Curve Subdivision for Application to High Performance Computing

K. E. Jordan[c], J. Li[a], T. J. Peters [1b], J. A. Roulier[b]

[a] *Department of Mathematics, University of Connecticut, Storrs.*
[b] *Department of Computer Science and Engineering, University of Connecticut, Storrs.*
[c] *Watson Research Center, IBM, Cambridge, MA.*

Abstract

For an arbitrary degree Bézier curve $\mathcal{B}$, we first establish sufficient conditions for its control polygon to become homeomorphic to $\mathcal{B}$ via subdivision. This is extended to show a subdivided control polygon that is ambient isotopic to $\mathcal{B}$. We provide closed-form formulas to compute the corresponding number of iterations for equivalence under homeomorphism and ambient isotopy. The development of these *a priori* values was motivated by application to high performance computing (HPC), where providing estimates of total run time is important for scheduling.

Keywords: Bézier curve, subdivision, piecewise linear approximation, non-self-intersection, homeomorphism, ambient isotopy.

2000 MSC: 57Q37, 57M50, 57Q55, 68R10

---

1. Introduction

Preserving ambient isotopic equivalence between an initial geometric model and its approximation is of contemporary interest in geometric modeling [1, 2, 4, 23, 27], with the focus here being on Bézier curves.

A Bézier curve is characterized by an indexed set of points, which form a piecewise linear (PL) approximation of the curve, called a control poly-

[1]This author was partially supported by NSF grants CCF 0429477, CMMI 1053077, CNS 0923158 and by IBM. All statements here are the responsibility of the author, not of the National Science Foundation nor of IBM.

gon (Definition 2.1). We consider the special class of *simple*[2] Bézier curves, because we are interested in knots[3].

1.1. Computational Topology Issues

The motivation for this theory was the scaling of dynamic visualization to HPC applications. For models of complex molecules [13], as found in the Protein Data Bank (PDB), Bézier curve models of these molecular backbones could be of arbitrarily high degree, but the existing literature on relevant ambient isotopic approximation was limited to degree 3 [27]. A formally proven *guarantee* that the graphics be ambient isotopic to the Bézier curve is essential. A simulation of molecular writhing is run on a high performance computing architecture, generating terabytes of floating point data. The output of all this data is the significant bottleneck. However, small portions of the data, covering seconds to minutes of the simulation can be offloaded within an acceptably minimal time lag to enable nearly synchronous dynamic visualization for informed decisions in computational steering. The appropriately high threshold here is that the dynamic visualization should not lead to inappropriate abortion of a simulation, based upon a misrepresentation of the isotopty type of the molecule.

There may be substantial topological differences between Bézier curves and their control polygons. It has long been known that Bézier curves and their control polygons are not necessarily homeomorphic. There are examples in the literature showing self-intersecting Bézier curves with simple control polygons or simple Bézier curves with self-intersecting control polygons [20, 31, 33]. Bézier curves and their control polygons are not necessarily ambient isotopic. There is an example showing an unknotted Bézier curve with a knotted control polygon [5, 26]. Examples of a knotted Bézier curve with an unknotted control polygon have also been given [20, 34].

The de Casteljau algorithm [12] is a subdivision algorithm associated to Bézier curves which recursively generates control polygons more closely approximating the curve under Hausdorff distance [29]. It is known that the convergence of the subdivided control polygon to its Bézier curve is exponential under Hausdorff distance [15, 30]. As a fundamental lemma, we show

[2]A curve is said to be simple if it is non-self-intersecting, exclusive of common end points of a closed curve and junction points in composite Bézier curves.

[3]A knot is a simple closed curve.

that the convergence of the exterior angles of the subdivided control polygon to 0 is also exponential for simple, regular, C^1, composite Bézier curves[4] in $\mathbb{R}^3$. Furthermore, we derive closed-form formulas to compute sufficient numbers of subdivision iterations to achieve homeomorphism and ambient isotopy, respectively.

1.2. Application to HPC Molecular Simulations

A brief overview of the relevant computational science issues follows. Prior knowledge of the run time of any job is important to estimate HPC time allocation and the sufficient number of iterations presented here will permit computational scientists to produce reliable estimates. With often more than 100,000 processors available, there are many creative, *ad hoc* parallelization techniques to achieve acceptable performance for subdivision. The initial ambient isotopic approximation can be done on a static geometric model, before the simulation begins. The next crucial experimental question is, "As the spline perturbs, how long can the original PL approximation be perturbed to maintain ambient isotopic equivalence?" Recently published work [7] provides some initial insight. If these time periods are sufficient for the amount of data initially output, then the cycle would begin again, but this remains to be verified experimentally. The emphasis here is that the theory proven here provides a strong foundation to pursue these experiments with confidence that subdivision will not become a time sink. As a contrast, in absence of this theory, the subdivision might be run recursively, with no prior knowledge of time to completion. The classical pipe surfaces was invoked as the boundary of a tubular neighborhood as an algorithmic constraint for a PL ambient isotopic approximation of a static spline curve [22]. That static view has been extended so that many perturbations of the PL approximant within the pipe surface continue to maintain ambient isotopic equivalence [13] and is applied here. Once the dynamic visualization begins, the containtment of the PL graphics within a pipe surface of constant radius enables run time warning messages, as the geometry approaches the boundary of this tubular neighborhood, increasing the prospect for a significant topological change. This is far superior to prevailing animation techniques that concentrate on self-intersection analysis on a per frame basis, which are known to be error prone [13, 17].

[4]These Bézier curves are necessarily compact, as continuous images of $[0, 1]$.

The availability of hundreds of thousands of processors noted in the preceding paragraph is common today. The number of processors is rapidly growing to millions, so moving simulation data results will become an issue of increasing greater concern. Computational steering and in-situ visualization will become ever more important. The theoretical results presented here provide the foundation to ensure that the perturbed PL graphics faithfully represent the underlying molecular science. The resultant algorithms are expected to scale gracefully. In the absence of this theory, an inappropriate steering decision – based upon a flawed visual analysis, could lead to lost results. These flawed decisions are expensive, motivating this theory as the primary basis for properly informed decisions.

2. Bézier Curves: Definitions and Assumptions

Some basic background on Bézier curves is provided.

Definition 2.1. *A parameterized **Bézier curve** of degree n with control points $p_j \in \mathbb{R}^3$ is defined by*

$$\sum_{j=0}^{n} B_{j,n}(t)p_j, t \in [0,1],$$

*where $B_{j,n}(t) = \binom{n}{j} t^j (1-t)^{n-j}$ and the PL curve given by the ordered set of points $\{p_0, p_1, \ldots, p_n\}$ is called its **control polygon** and is denoted by P. When $p_0 = p_n$, the control polygon is closed. Otherwise when $p_0 \neq p_n$, it is open.*

In order to avoid technical considerations and to simplify the exposition, the class of Bézier curves considered will be restricted to those where the first derivative never vanishes.

Definition 2.2. *A differentiable curve is said to be **regular** if its first derivative never vanishes.*

The Bézier curve of Definition 2.1 is typically called a *single segment Bézier curve*, while a *composite Bézier curve* is created by joining a sequence of two or more single segment open Bézier curves at their common end points.

Throughout the paper, we use $\mathcal{B}$ to denote a simple, regular, C^1, composite Bézier curve

$$\mathcal{B} : [0,1] \rightarrow \mathbb{R}^3,$$

defined by a control polygon with distinct consecutive vertices, except that for a closed Bézier curve, the end points are the same.

Beginning with Theorem 6.2 the hypothesis of C^2 is added for $\mathcal{B}$, but this is because the C^2 condition was previously implicitly used in establishing a non-singular pipe surface [22] as the boundary of a tubular neighborhood. This dependency continues for other results which use this non-singular pipe. This non-singular pipe surface is merely a convenience to ease the exposition. There are many cases where the C^1 assumption will suffice for an alternative tubular neighborhood to replace that created with the indicated pipe surface as its boundary. Some creative alternatives could rely upon previous 'snow cone' constructions [14], but this is left as a subject of future work. We note that our use of Fenchel's Theorem 4.1 in the proof of Lemma 6.2 relies only on the PL case.

3. Related Work

Exponential convergence in Hausdorff distance of the subdivided control polygon to its Bézier curve under subdivision has previously been established [15, 30]. The discrete derivatives of the control polygons were proven to converge exponentially to the derivatives of the Bézier curve by showing that discrete differentiation commutes with subdivision [28]. The convergence of the exterior angles of the subdivided control polygons to 0 has been widely assumed, both in the literature [16] and informally, but we were unable to find any proof in the literature. We prove this angular convergence, using derivatives.

The *existence* of homeomorphic equivalence between a sufficiently fine subdivided control polygon and its Bézier curve was given [31] by invoking the hodograph[5], but that proof provided no expression for the number of subdivision iterations. We provide a constructive geometric proof for specified

[5]The derivative of a Bézier curve is also expressed as a Bézier curve, known as the *hodograph* [12].

numbers of subdivision iterations to produce a control polygon homeomorphic to a given Bézier curve. We then extend to a similar result for ambient isotopy.

The *a priori* determination of the number of iterations was motivated by experimental performance studies for dynamic visualization in molecular simulations, where the molecules are modeled as knots. Homeomorphic approximation of composite Bézier curves was established [9] by algorithmic techniques that do not directly rely upon the de Casteljau algorithm, but include techniques related to "significant points". The self-intersection of curves and surfaces is fundamental within geometric modeling [3, 32]. Preservation of topology was established when the control points of parametric patches are perturbed, by designating conditions under which perturbations yield no self-intersections of patches [4].

Our techniques rely upon a tubular neighborhood for a Bézier curve, with the boundary of the tubular neighborhood being a non-singular pipe surface. Pipe surfaces have been studied since the 19th century [25], but the presentation here follows a contemporary source [22]. These authors perform a thorough analysis and description of the end conditions of open spline curves. The junction points of a Bézier curve are merely a special case of that analysis.

Ambient isotopy is a stronger notion of equivalence than homeomorphism. An earlier algorithm [14] establishes an isotopic approximation over a broad class of parametric geometry, without establishing the number of iterations needed. Other recent papers [6, 21] present algorithms to compute isotopic PL approximation for $2D$ algebraic curves. Computational techniques for establishing isotopy and homotopy have been established regarding algorithms for point-clouds by "distance-like functions" [8].

Ambient isotopy under subdivision was previously established [27] for $3D$ Bézier curves of low degree (less than 4), where a crucial unknotting condition was trivially established for these low degrees. The results presented here extend to Bézier curves of arbitrary degree, by a more refined analysis of avoiding knots locally within the PL approximation generated. The focus on higher degree versions was motivated by applications in molecular simulation.

It was proved that for homeomorphic curves, if their distance and angles between first derivatives are within given bounds, then these curves are ambient isotopic [10]. We invoke this previous result.

4. Mathematical Preliminaries

Mathematical definitions, notation and fundamental supportive results are presented in this section. More specialized definitions will follow in appropriate sections. The standard Euclidean norm will be denoted by $|| \quad ||$.

Definition 4.1. *A C^1 function, f, is $C^{1,1}$ if its derivative, denoted by f' is Lipshitz.*

Lemma 4.1. *The curve $\mathcal{B}$ is $C^{1,1}$.*

Proof: The proof relies upon $\mathcal{B}$ being C^1 and invokes the Mean Value Theorem, the definition of a single segment Bézier curve by a polynomial, the differentiability of a polynomial and the existence of the maximum of any continuous real valued function on a compact domain. The elementary details are left to the reader. □

Definition 4.2. [29] *Let X and Y be two non-empty subsets of a metric space (M, d). The **Hausdorff distance** $\mu(X, Y)$ is defined by*

$$\mu(X,Y) := \max\{\sup_{x \in X} \inf_{y \in Y} d(x,y), \sup_{y \in Y} \inf_{x \in X} d(x,y)\}.$$

Subdivision algorithms are fundamental for Bézier curves and a brief overview is given here. Figure 1 shows the first step of the de Casteljau algorithm with an input value of $\frac{1}{2}$ on a single Bézier curve. For ease of exposition, the de Casteljau algorithm with this value of $\frac{1}{2}$ is assumed, but other fractional values can be used with appropriate minor modifications to the analyses presented. The initial control polygon P is used as input to generate local PL approximations, P^1 and P^2, as Figure 1(b) shows. They together form a new PL curve whose Hausdorff distance is closer to the curve than that of P [12].

A summary is that subdivision proceeds by selecting the midpoint of each edge of P and these midpoints are connected to create new edges, as Figure 1(a) shows. Recursive creation and connection of midpoints continues until a single edge is created, which is, in fact, tangent to the Bézier curve [12]. The union of the edges from the final step then forms a new PL curve. Termination is guaranteed since P has only finitely many edges.

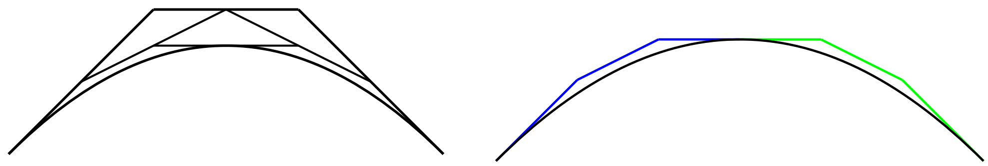

(a) Subdivision process (b) P^1 and P^2

Figure 1: A subdivision with parameter $\frac{1}{2}$

For a single segment curve, after i iterations[6], the subdivision process generates 2^i PL sub-curves, each being a control polygon for part of the original curve [12], which is a **sub-control polygon**[7] (For simplicity, it will be referred to as **sub-polygon**), denoted by P^k for $k = 1, 2, 3, \ldots, 2^i$. Each P^k has $n + 1$ points and their union $\bigcup_k P^k$ forms a new PL curve that converges in Hausdorff distance to approximate the original Bézier curve. The Bézier curve defined by $\bigcup_k P^k$ is exactly the same Bézier curve defined by the original control points $\{p_0, p_1, \ldots, p_n\}$ [15]. So $\bigcup_k P^k$ is a new control polygon of the Bézier curve. We will consistently just shorten $\bigcup_k \mathcal{P}^k$ to $\mathcal{P}_i(t)$ for the subdivided polygon after i iterations.

Exterior angles were defined [24] in the context of closed PL curves, but are adapted here for both closed and open PL curves. Exterior angles unify the concept of total curvature for curves that are PL or differentiable.

Definition 4.3. [24] *The **exterior angle** between two oriented line segments, denoted as $\overrightarrow{p_{j-1}p_j}$ and $\overrightarrow{p_jp_{j+1}}$, where $p_{j-1} \neq p_j$ and $p_j \neq p_{j+1}$, is the angle formed by $\overrightarrow{p_jp_{j+1}}$ and the extension of $\overrightarrow{p_{j-1}p_j}$. Let the measure of the exterior angle be α_j satisfying:*

$$0 \leq \alpha_j \leq \pi.$$

Definition 4.4. *Parametrize a curve $\gamma(s)$ with arc length s on $[0, \ell]$. Then its **total curvature** is $\int_0^\ell ||\gamma''(s)||\, ds$.*

[6] An iteration is a whole subdivision process that produces a new control polygon.

[7] Note that by the subdivision process, each sub-control polygon of a simple Bézier curve is open.

Total curvature can be defined for both C^2 and PL curves. In both cases, the total curvature is denoted by $T_\kappa(\cdot)$. The unified terminology is invoked in Fenchel's theorem, which is fundamental to the work presented here.

Definition 4.5. [24] *Suppose that a PL curve in $\mathbb{R}^3$, denoted by Q, is defined by an ordered set of points $\{q_0, q_1, \ldots, q_n\}$ where $q_j \neq q_{j+1}$ for $j = 0, 1, \ldots, n-1$, then the **total curvature** of Q is the sum of the measures of all the exterior angles.*

Fenchel's Theorem [11] presented below is applicable both to PL curves and to differentiable curves.

Theorem 4.1. [11, Fenchel's Theorem] *The total curvature of any closed curve is at least 2π, with equality holding if and only if the curve is planar and convex.*

Denote a PL curve with vertices $\{q_0, q_1, \ldots, q_n\}$ by Q, and the uniform parametrization [28] of Q over $[0, 1]$ by $l(Q)_{[0,1]}$. That is:

$$l(Q)_{[0,1]}\left(\frac{j}{n}\right) = q_j \; for \; j = 0, 1, \cdots, n$$

and $l(Q)_{[0,1]}(t)$ interpolates linearly between vertices.

Definition 4.6. *First define discrete derivatives [28] at the parameters $t_j = \frac{j}{n}$, where*

$$l(Q)_{[0,1]}(t_j) = q_j, \; for \; j = 0, 1, \cdots, n-1.$$

Let

$$q'_j = l'(Q)_{[0,1]}(t_j) = \frac{q_{j+1} - q_j}{t_{j+1} - t_j}, \; for \; j = 0, 1, \cdots, n-1.$$

*Denote $Q' = (q'_0, q'_1, \ldots, q'_{n-1})$. Then define the **discrete derivatives** for $l(Q)_{[0,1]}$ as:*

$$l'(Q)_{[0,1]} = l(Q')_{[0,1]}.$$

5. Angular Convergence under Subdivision

For simplicity of notation, use $\mathcal{P}_0(t)$ to denote the original control polygon before subdivision, which is uniformly parameterized, that is, $\mathcal{P}_0(t) = l(P)_{[0,1]}$. Let M be the maximum of the distance between two consecutive vertices of the first discrete derivative of $\mathcal{P}_0(t)$. Similarly, we use $\mathcal{P}(t)$ to denote a subdivided control polygon, uniformly parametrized over $[0,1]$. Let $\mathcal{P}'(t)$ be the corresponding discrete derivative. Let $\mathcal{P}(t_{j-1})$ and $\mathcal{P}(t_j)$, for $j = 1, 2, \ldots, n$, be any consecutive vertices of $\mathcal{P}(t)$.

Lemma 5.1. *For the curve $\mathcal{B}$, we have*

$$||\mathcal{P}'(t_j) - \mathcal{P}'(t_{j-1})|| \leq \frac{M}{2^i}.$$

Proof: It was proved that the discrete differentiation commutes with subdivision [28, Lemma 4], so $\mathcal{P}'$ can be viewed as being obtained by subdividing $\mathcal{P}_0'$. But $\mathcal{P}_0'$ is a control polygon of $\mathcal{B}'$ [28, Lemma 6]. Another previous result [15, Lemma 2.5] showed that the distance between any two consecutive vertices of a control polygon is bounded by $\frac{M}{2^i}$. □

Theorem 5.1 (Angular Convergence). *For $\mathcal{B}$, the exterior angles of the PL curves generated by subdivision converge uniformly to 0 at a rate of $O\left(\sqrt{\frac{1}{2^i}}\right)$.*

Proof: Since $\mathcal{B}(t)$ is assumed to be regular and C^1, the non-zero minimum of $||\mathcal{B}'(t)||$ over the compact set [0,1] is attained. For brevity, the notations of $u_j = \mathcal{P}'(t_j)$, $v_j = \mathcal{P}'(t_{j-1})$ and $\alpha = \alpha_j$ are introduced. The convergence of u_j to $\mathcal{B}'(t_j)$ [28] implies that $||u_j||$ has a positive lower bound (denoted by λ), for the number of subdivision iterations, i, sufficiently large.

Lemma 5.1 gives that $||u_j - v_j|| \to 0$ as $i \to \infty$ at a rate of $O(\frac{1}{2^i})$. This implies: $||u_j|| - ||v_j|| \to 0$ as $i \to \infty$ at a rate of $O(\frac{1}{2^i})$.

Consider

$$1 - \cos(\alpha) = 1 - \frac{u_j v_j}{||u_j|| \cdot ||v_j||}$$

$$= \frac{||u_j|| \cdot ||v_j|| - v_j v_j + v_j v_j - u_j v_j}{||u_j|| \cdot ||v_j||}$$

$$\leq \frac{||u_j|| - ||v_j||}{||u_j||} + \frac{||v_j - u_j||}{||u_j||} \leq \frac{||u_j|| - ||v_j||}{\lambda} + \frac{||v_j - u_j||}{\lambda} \leq \frac{2||v_j - u_j||}{\lambda} \tag{1}$$

It follows from Lemma 5.1 that

$$1 - \cos(\alpha) \leq \frac{M}{\lambda 2^{i-1}}. \tag{2}$$

It follows from the continuity of $arc\cos$ that α converges to 0 as $i \to \infty$. To obtain the convergence rate, taking the power series expansion of cos we get

$$\begin{aligned} 1 - \cos(\alpha) &\geq \alpha^2 \left(\frac{1}{2} - \left| \frac{\alpha^2}{4!} - \frac{\alpha^4}{6!} + \cdots \right| \right) \\ &= \alpha^2 \left(\frac{1}{2} - \alpha^2 \left| \frac{1}{4!} - \frac{\alpha^2}{6!} + \cdots \right| \right). \end{aligned} \tag{3}$$

Note that for $1 > \alpha$,

$$e = 1 + 1 + \frac{1}{2!} + \frac{1}{3!} + \frac{1}{4!} + \cdots > \left| \frac{1}{4!} - \frac{\alpha^2}{6!} + \cdots \right|. \tag{4}$$

Combining (3) and (4) we have,

$$1 - \cos(\alpha) > \alpha^2 \left(\frac{1}{2} - \alpha^2 e \right).$$

For any $\tau \in \left(0, \frac{1}{2}\right)$, sufficiently many subdivisions will guarantee that α is small enough such that $1 > \alpha$ and $\tau > \alpha^2 e$. Thus

$$1 - \cos(\alpha) > \alpha^2 \left(\frac{1}{2} - \alpha^2 e \right) > \alpha^2 \left(\frac{1}{2} - \tau \right) > 0.$$

By (2) we have

$$\alpha < \sqrt{\frac{2M}{\lambda(\frac{1}{2} - \tau)}} \sqrt{\frac{1}{2^i}}.$$

So α converges to 0 at a rate of $O\left(\sqrt{\frac{1}{2^i}}\right)$. □

6. Homeomorphic Control Polygons

We present sufficient conditions for a homeomorphism between a subdivided control polygon and $\mathcal{B}$. We first establish a local homeomorphism between a sub-polygon and the corresponding sub-curve of $\mathcal{B}$, and then establish a global homeomorphism between the control polygon and $\mathcal{B}$.

Lemma 6.1. [16, Angle criterion] *Let Q be an open PL curve in $\mathbb{R}^3$. If $T_\kappa(Q) = \sum_{j=1}^{n-1} \alpha_j < \pi$, then Q is simple.*

Theorem 6.1. *For $\mathcal{B}$, there exists a sufficiently large value of i, such that after i-many subdivisions, each of the sub-polygons generated as P^k for $k = 1, 2, 3, \ldots, 2^i$ will be simple.*

Proof: The measures of the exterior angles of P^k converge uniformly to zero as i increases (Theorem 5.1). Each open P^k has n edges. Denote the $n-1$ exterior angles of each P^k by α_j^k, for $j = 1, \ldots, n-1$ and for $k = 1, 2, 3, \ldots, 2^i$. Then there exists i sufficiently large such that

$$\sum_{j=1}^{n-1} \alpha_j^k < \pi,$$

for each $k = 1, 2, 3, \ldots, 2^i$. Use of Lemma 6.1 completes the proof. □

The proof techniques for homeomorphism rely upon the sub-polygons to be pair wise disjoint, except at their common end points. Denote two generated sub-polygons of $\mathcal{B}$ as

$$P = (p_0, p_1, \ldots, p_n) \text{ and } Q = (q_0, q_1, \ldots, q_m).$$

Definition 6.1. *The sub-polygons P and Q are said to be **consecutive** if the last vertex p_n of P is the first vertex q_0 of Q, that is, $p_n = q_0$.*

Remark 6.1. *For $\mathcal{B}$, the C^2 assumption ensures that the segments $\overrightarrow{p_{n-1}p_n}$ and $\overrightarrow{q_0q_1}$ are collinear. The regularity assumption ensures that the exterior angle can not be π. So the exterior angle at the common point is 0.*

Lemma 6.2 extends to arbitrary degree Bézier curves from a previously established result that was restricted to cubic Bézier curves [35], as used in the proof of isotopy under subdivision for low-degree Bézier curves [27].

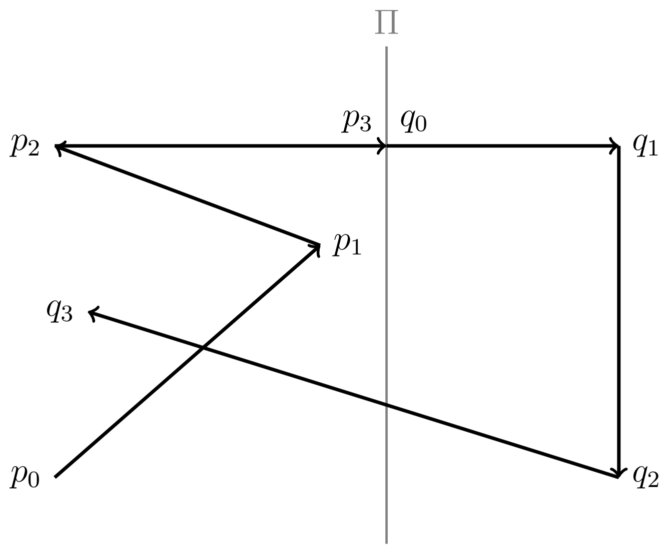

Figure 2: Intersecting consecutive sub-polygons

Lemma 6.2. *Let* Π *be the plane normal to a sub-polygon at its initial vertex. If the total curvature of the sub-polygon is less than* $\frac{\pi}{2}$*, then the initial vertex is the only point where the plane intersects the sub-polygon.*

Proof: Denote the sub-polygon as $Q = (q_0, q_1, \ldots, q_m)$, where $q_j \neq q_{j+1}$, $j = 0, 1, \ldots, m-1$. Figure 2 shows an orthogonal projection of this 3D geometry in the case $n = m = 3$. Assume to the contrary that $\Pi \cap Q$ contains a point u where $u \neq q_0$. Consider the closed polygon formed by vertices $\{q_0, \ldots, u, q_0\}$. Then by Theorem 4.1 we know that the total curvature of the closed polygon is at least 2π. However, excluding the exterior angles at q_0 (which is $\frac{\pi}{2}$), and the exterior angles at u (which is at most π by Definition 4.3), we still have at least $\frac{\pi}{2}$ left, which contradicts $T_\kappa(Q) < \frac{\pi}{2}$. $\square$

Lemma 6.3. *Let* w *be a point of* $\mathcal{B}$ *where* $\mathcal{B}$ *is subdivided, that is,* w *is the common point of two connected sub-polygons, and let* Π *be the plane normal to* $\mathcal{B}$ *at* w*. Then there exists a subdivision of* $\mathcal{B}$ *such that the sub-polygon ending at* w *and the sub-polygon beginning at* w *intersect* Π *only at the point* w*.*

Proof: The plane Π separates the space $\mathbb{R}^3$ into two disjoint open half-spaces, denoted as H_1 and H_2, such that

$$H_1 \cup \Pi \cup H_2 = \mathbb{R}^3 \text{ and } H_1 \cap H_2 = \emptyset.$$

By Remark 6.1, the exterior angle at w is 0.

Perform sufficiently many subdivisions so that the control polygon ending at w, denoted by P, and the control polygon beginning at w, denoted by Q, each have total curvature less than $\frac{\pi}{2}$ (Theorem 5.1). Therefore, by Lemma 6.2 the only point where P or Q intersect Π is at w. □

This global homeomorphism will be proven by reliance upon pipe surfaces, which are defined below.

Definition 6.2. *The* ***pipe surface*** *of radius r of a parameterized curve $\boldsymbol{c}(t)$, where $t \in [0, 1]$ is given by*

$$\boldsymbol{p}(t, \theta) = \boldsymbol{c}(t) + r[cos(\theta)\ \boldsymbol{n}(t) + sin(\theta)\ \boldsymbol{b}(t)],$$

where $\theta \in [0, 2\pi]$ and $\boldsymbol{n}(t)$ and $\boldsymbol{b}(t)$ are, respectively, the normal and binormal vectors at the point $\boldsymbol{c}(t)$, as given by the Frenet-Serret trihedron. The curve $\mathbf{c}$ is called a spine curve.

For $\mathcal{B}$ and i subdivisions, with resulting sub-polygons P^k for $k = 1, \ldots, 2^i$, let $S_r(\mathcal{B})$ be a pipe surface of radius r for $\mathcal{B}$ so that $S_r(\mathcal{B})$ is non-self-intersecting. Theorem 3.1 in [22] ensures the existence of such a non-self-intersecting pipe surface. For each $k = 1, \ldots, 2^i$, denote

- the parameter of the initial point of P^k by t_0^k, and that of the terminal point by t_n^k
- the normal disc of radius r centered at $\mathcal{B}(t)$ as $D_r(t)$,
- the union $\bigcup_{t \in [t_0^k, t_n^k]} D_r(t)$ by Γ_k, and designate it as a **pipe section**.

Theorem 6.2. *If $\mathcal{B}$ is C^2, then sufficiently many subdivisions will yield a simple control polygon that is homeomorphic to $\mathcal{B}$.*

Proof: By Theorem 5.1, we can take ι_1 subdivisions so that $T_\kappa(P^k) < \pi/2$, for each sub-polygon P^k. By Lemma 6.1, this choice of ι_1 guarantees that each P^k is simple. By the convergence in Hausdorff distance under subdivision [30], we can take ι_2 subdivisions such that the control polygon generated by ι_2 subdivision fits inside the non-singular pipe surface $S_r(\mathcal{B})$ [22]. Choose $\iota = \max\{\iota_1, \iota_2\}$. By Lemma 6.3, this choice of ι ensures that each P^k fits inside the corresponding Γ_k, so that the control polygon, $\bigcup_{k=1}^{2^i} P^k$, is simple, which implies the homeomorphism. □

7. Ambient Isotopic Control Polygons

Ambient isotopy is an equivalence relation for knots. Knots can be modeled by simple closed Bézier curves. In this section, we consider a closed Bézier curve $\mathcal{B}$, and derive the ambient isotopy following [10, Proposition 3.1]. We note that $C^{1,1}$ was previously used [10], which is true for $\mathcal{B}$ by Corollary 4.1. The stronger C^2 assumption invoked, below, is to ensure the singularity of the pipe surface, as previously noted in Section 2.

Theorem 7.1. *If $\mathcal{B}$ is C^2, then sufficiently many subdivisions will yield a simple control polygon that is ambient isotopic to $\mathcal{B}$.*

Proof: It was proved [10, Proposition 3.1] that $\mathcal{B}$ and $\mathcal{P}$ are ambient isotopic if:

(1) they are homeomorphic,
(2) $||\mathcal{B}(t) - \mathcal{P}(t)|| < \frac{r}{2}$ (where r is the radius of a pipe surface), and
(3) $\max_{t\in[0,1]} \theta(t) < \frac{\pi}{6}$ (where $\theta(t)$ is the angle between $\mathcal{B}'(t)$ and $\mathcal{P}'(t)$).

By Theorem 6.2, sufficiently many subdivisions will produce a homeomorphic $\mathcal{P}$. Also, $\mathcal{P}(t)$ converges to $\mathcal{B}(t)$ [30] and $\mathcal{P}'(t)$ converges to $\mathcal{B}'(t)$ [28]. Therefore, the conclusion follows. □

8. Sufficient Subdivision Iterations

In this section, we shall establish closed-form formulas to compute sufficient numbers of subdivisions for small exterior angles, homeomorphism and ambient isotopy respectively.

From the previous sections we know that the homeomorphism is obtained by subdivision based on two criteria:

(1) angular convergence; and
(2) convergence in distance.

So the speed of achieving these topological characteristics is determined by the angular convergence rate and the convergence rate in distance which are both exponential. Here, we further find closed-form formulas to compute sufficient numbers of subdivision iterations to achieve these properties.

Definition 8.1. *Let P denote a control polygon of a Bézier curve, and let P_x denote an ordered list of all of x-coordinates of P (with similar meaning given to P_y for the y-coordinates and to P_z for the z-coordinates). Let*

$$\| \triangle_2 P_x \|_\infty = \max_{0<m<n} |P_{m-1,x} - 2P_{m,x} + P_{m+1,x}|$$

be the maximum absolute second difference of the x-coordinates of control points, (with similar meanings for the y and z coordinates) . Let

$$\Delta_2 P = (\| \triangle_2 P_x \|_\infty, \| \triangle_2 P_y \|_\infty, \| \triangle_2 P_z \|_\infty),$$

(i.e.) a vector with 3 values.

Definition 8.2. *The distance*[8] [30] *between a Bézier curve $\mathcal{B}$ and the control polygon $\mathcal{P}$ generated by i subdivisions is given by*

$$\max_{t \in [0,1]} ||\mathcal{P}(t) - \mathcal{B}(t)||.$$

Lemma 8.1. *The distance between the Bézier curve and its control polygon after ith-round subdivision has an upper bound of*

$$\frac{1}{2^{2i}} N_\infty(n) ||\Delta_2 P||, \tag{5}$$

where

$$N_\infty(n) = \frac{\lfloor n/2 \rfloor \cdot \lceil n/2 \rceil}{2n}.$$

Proof: A published lemma [30, Lemma 6.2] proves a similar result restricted to scalar valued polynomials. We consider coordinate-wise and apply this result to the x, y, and z coordinates respectively, so that the distance of the x-coordinates of the Bézier curve and its control polygon after ith-round subdivision is bounded by

$$\frac{1}{2^{2i}} N_\infty(n) \parallel \Delta_2 P_x \parallel_\infty,$$

[8] The distance here is as previously used [30]. Note that the distance is not smaller than Fréchet distance. Our following results remain true if this distance is changed to Fréchet distance.

with similar expressions for the y and z coordinates. Taking the Euclidean norm of the indicated three x, y and z bounds yields the upper bound given by (5), an upper bound of the distance between the Bézier curve and its control polygon after the ith subdivision. □

For convenience, denote the upper bound in distance as:

$$B_{dist}(i) := \frac{1}{2^{2i}} N_\infty(n) ||\Delta_2 P||. \tag{6}$$

Lemma 8.2. *After i subdivision iterations, the distance between $\mathcal{P}'$ and $\mathcal{B}'$ has an upper bound of $B'_{dist}(i)$, where*

$$B'_{dist}(i) := \frac{1}{2^{2i}} N_\infty(n-1) ||\Delta_2 P'||, \tag{7}$$

and P' that consists of $n-1$ control points is the control polygon of $\mathcal{B}'$.

Proof: A control polygon's derivative is again a control polygon of the Bézier curve's derivative [28, Lemma 6]. So by Lemma 8.1, we have

$$\max_{t\in[0,1]} ||\mathcal{P}'(t) - \mathcal{B}'(t)|| \leq B'_{dist}(i). \tag{8}$$

□

8.1. Subdivision iterations for small exterior angles

Assume ν is a small measure of angle between 0 and π. We shall find how many subdivisions will generate a control polygon such that the measure α of each exterior angle satisfies[9]

$$\alpha < \nu. \tag{9}$$

Recall the proof of angular convergence (Theorem 5.1). Consider two arbitrary consecutive derivatives $u_j = \mathcal{P}'(t_j)$ and $v_j = \mathcal{P}'(t_{j-1})$ and the corresponding exterior angle α. Recall that in Section 5 we had (1) and (2):

$$1 - \cos(\alpha) \leq \frac{2||v_j - u_j||}{||u_j||} \leq \frac{M}{||u_j|| 2^{i-1}}. \tag{10}$$

[9]Later, in Sections 8.2 and 8.3, we shall see that the size of ν depends on the degree n of a Bézier curve.

Let $\sigma = \min\{||\mathcal{B}'(t)|| : t \in [0,1]\}$. The regularity of $\mathcal{B}$ ensures that $\sigma > 0$ and the continuity of $\mathcal{B}'$ on the compact interval $[0,1]$ ensures that the minimum exists. It follows from (8) that

$$||\mathcal{B}'(t_j)|| - ||u_j|| \leq B'_{dist}(i).$$

Solving the inequality we get

$$||u_j|| \geq ||\mathcal{B}'(t_j)|| - B'_{dist}(i) \geq \sigma - B'_{dist}(i).$$

In order to have $u_j \neq 0$, it is sufficient to perform enough subdivisions such that

$$||u_j|| \geq \sigma - B'_{dist}(i) > 0,$$

that is $B'_{dist}(i) < \sigma$. By the definition of $B'_{dist}(i)$, given by (7), we set,

$$\frac{1}{2^{2i}} N_\infty(n-1) \parallel \triangle_2 P' \parallel < \sigma.$$

Therefore for $B'_{dist}(i) < \sigma$, it suffices to have[10]

$$i > \frac{1}{2}\log\left(\frac{N_\infty(n-1) \parallel \triangle_2 P' \parallel}{\sigma}\right) = N_1. \tag{11}$$

After the i subdivision iterations for $i > N_1$, $B'_{dist}(i) < B'_{dist}(N_1)$, because $B'_{dist}(i)$ is a strictly decreasing function. So it follows from (10) that whenever $i > N_1$,

$$1 - \cos(\alpha) \leq \frac{M}{2^{i-1}(\sigma - B'_{dist}(i))}.$$

To obtain $\alpha < \nu$, it suffices to have that

$$1 - cos(\alpha) < 1 - cos(\nu).$$

Now choose i large enough so that

$$1 - \cos(\alpha) \leq \frac{M}{2^{i-1}(\sigma - B'_{dist}(N_1))} < 1 - \cos(\nu). \tag{12}$$

[10]Throughout this paper, we use log for $\log_2$.

The second inequality of (12) implies that

$$i > \log\left(\frac{2M}{(1-\cos(\nu))(\sigma - B'_{dist}(N_1))}\right).$$

To simplify this expression, let

$$f(\nu) = \frac{2M}{(1-\cos(\nu))(\sigma - B'_{dist}(N_1))}. \tag{13}$$

Then, we have

$$i > \log(f(\nu)).$$

Theorem 8.1. *Given any $\nu > 0$, consider the integer $N(\nu)$ defined by*

$$N(\nu) = \lceil \max\{N_1, \log(f(\nu))\} \rceil \tag{14}$$

where N_1, and $f(\nu)$ are given by (11) and (13) respectively. If $i > N(\nu)$, then each exterior angle is less than ν.

Proof: It follows from the definitions of N_1 and $f(\nu)$ and the above analysis. $\square$

It is worth noting that N is a logarithm depending on several parameters such as σ, $N_\infty(n)$ and $\triangle_2 P'$ as well as the variable ν.

8.2. Subdivision iterations for homeomorphism

For a regular simple Bézier curve $\mathcal{B}$ of degree 1 or 2, the control polygon is trivially[11] ambient isotopic to $\mathcal{B}$. We consider $n \geq 3$.

Given any $\nu > 0$, Theorem 8.1 shows that there exists an integer $N(\nu)$, such that each exterior angle is less than ν after $N(\nu)$ subdivisions. Furthermore, there is an explicit closed formula to compute $N(\nu)$.

Theorem 8.2. *There exists a positive integer, $N(\frac{\pi}{n-1})$ for $n > 2$, where $N(\frac{\pi}{n-1})$ is defined by (14), such that after $\lceil N(\frac{\pi}{n-1}) \rceil$ subdivisions, each subpolygon will be simple.*

[11] For degree 1, both the curve and the polygon are either a point or a line segment. For degree 2, there are three points. The curve and the polygon are planar and open (otherwise the curve is not regular).

Proof: By Theorem 8.1, after $N(\frac{\pi}{n-1})$ subdivisions, each exterior angle is less than $\frac{\pi}{n-1}$. Since each sub-polygon has a $n-1$ exterior angles, the total curvature of each sub-polygon is less than π. Lemma 6.1 implies that this is a sufficient condition for each sub-polygon being simple. □

Define $N'(r)$ by

$$N'(r) = \frac{1}{2}\log\left(\frac{N_\infty(n)||\Delta_2 P||}{r}\right), \tag{15}$$

where r is the radius of a non-self-intersecting pipe surface for $\mathcal{B}$. By (6) and (15), we have $B_{dist}(i) < r$ whenever $i > N'(r)$.

Lemma 8.3. *The control polygon generated by more than $N'(r)$ subdivision iterations, where $N'(r)$ is given by (15), satisfies*

$$\max_{t\in[0,1]} ||\mathcal{B}(t) - \mathcal{P}(t)|| < r,$$

and hence fits inside the pipe surface of radius r for $\mathcal{B}$.

Proof: By Lemma 8.1, $\max_{t\in[0,1]} ||\mathcal{B}(t) - \mathcal{P}(t)|| \leq B_{dist}(i)$. Then this lemma follows from the definition of $N'(r)$ given by (15). □

While Theorem 8.2 addresses each sub-polygon, it is of interest to ensure that the union of all these sub-polygons is also simple. In Theorem 8.3, that union is the 'control polygon', as the result of multiple subdivisions.

Theorem 8.3. *Set*

$$\hat{N} = \max\{N\left(\frac{\pi}{2(n-1)}\right), N'(r)\},$$

where $N(\nu)$ is defined by (14) and $N'(r)$ is given by (15). After $\lceil \hat{N} \rceil$ or more subdivisions, the control polygon will be homeomorphic.

Proof: The inequality $N \geq N'(r)$ implies that the control polygon generated after the N'th subdivision lies inside the pipe. The inequality $N \geq N\left(\frac{\pi}{2(n-1)}\right)$ ensures that the total curvature of its each sub-polygon is less than $\frac{\pi}{2}$. These two conditions are sufficient conditions for the control polygon being simple (Theorem 6.2). □

8.3. Subdivision iterations for ambient isotopy

Recall, by Theorem 7.1, that a a subdivided control polygon $\mathcal{P}$ that is homeomorphic to its Bézier curve $\mathcal{B}$ will also be ambient isotopic to$\mathcal{B}$ if

$$||\mathcal{B}(t) - \mathcal{P}(t)|| < \frac{r}{2} \text{ and } \max_{t \in [0,1]} \theta(t) < \frac{\pi}{6},$$

where $\theta(t)$ is the angle between $\mathcal{B}'(t)$ and $\mathcal{P}'(t)$. We may produce $N'\left(\frac{r}{2}\right)$ subdivisions to satisfy the first condition (Lemma 8.3). To guarantee the second condition, we consider:

$$1 - \cos(\theta(t)) = 1 - \frac{\mathcal{B}'(t) \cdot \mathcal{P}'(t)}{||\mathcal{B}'(t)|| \cdot ||\mathcal{P}'(t)||}$$
$$= \frac{||\mathcal{B}'(t)|| \cdot ||\mathcal{P}'(t)|| - \mathcal{P}'(t) \cdot \mathcal{P}'(t) + \mathcal{P}'(t) \cdot \mathcal{P}'(t) - \mathcal{B}'(t) \cdot \mathcal{P}'(t)}{||\mathcal{B}'(t)|| \cdot ||\mathcal{P}'(t)||}$$
$$\leq \frac{||\mathcal{B}'(t)|| - ||\mathcal{P}'(t)||}{||\mathcal{B}'(t)||} + \frac{||\mathcal{B}'(t) - \mathcal{P}'(t)||}{||\mathcal{B}'(t)||} \leq \frac{2||\mathcal{B}'(t) - \mathcal{P}'(t)||}{\sigma},$$

where $\sigma = \min\{||\mathcal{B}'(t)|| : t \in [0,1]\}$ (Recall $\sigma > 0$.) From (8)

$$\max_{t \in [0,1]} ||\mathcal{B}'(t) - \mathcal{P}'(t)|| \leq B'_{dist}(i),$$

we have

$$1 - \cos(\theta(t)) \leq \frac{2B'_{dist}(i)}{\sigma}.$$

To have $\theta(t) < \frac{\pi}{6}$, it suffices to set

$$\frac{2B'_{dist}(i)}{\sigma} < 1 - \cos(\frac{\pi}{6}) = 1 - \frac{\sqrt{3}}{2}.$$

By Equality 7,

$$B'_{dist}(i) := \frac{1}{2^{2i}} N_\infty (n-1) ||\Delta_2 P'||,$$

we get

$$i \geq \frac{1}{2} \log \left(\frac{2N_\infty(n-1)||\Delta_2 P'||}{(1 - \frac{\sqrt{3}}{2})\sigma} \right) = N_2. \qquad (16)$$

So N_2 subdivision iterations will guarantee the second condition.

Theorem 8.4. *Set*

$$N^* = \max\{N\left(\frac{\pi}{2(n-1)}\right), N'\left(\frac{r}{2}\right), N_2\},$$

where N, N', N_2 are given by (14), (15) and (16) respectively. After $\lceil N^* \rceil$ or more subdivisions, the control polygon $\mathcal{P}$ will be ambient isotopic to the Bézier curve $\mathcal{B}$.

Proof: The values $N\left(\frac{\pi}{2(n-1)}\right)$ and $N'(\frac{r}{2})$ are used to obtain a homeomorphism, by Theorem 8.3. And then N_2 is used to further obtain an ambient isotopy. □

Remark 8.1. *Note that $N\left(\frac{\pi}{2(n-1)}\right) = \max\{N_1, \log f(\frac{\pi}{2(n-1)})\}$. Comparing N_1 given by (11) and N_2 given by (16), we get that $N_2 < N_1 + 2$. By (15) we also have $N'\left(\frac{r}{2}\right) < N'(r) + 1$. So $N^* < \hat{N} + 2$. (Here, $\hat{N} = \max\{N\left(\frac{\pi}{2(n-1)}\right), N'(r)\}$ is a sufficient number of subdivisions to guarantee homeomorphism.) So after a homeomorphism based on Theorem 8.3 is attained, no more than 2 additional subdivision iterations will be used to produce the ambient isotopy*[12].

9. Future Work

The results here are restricted to uniform subdivision. Adaptive subdivision may well be appropriate and the methods presented here would form the basis for extension to adaptive methods, where different tubular neighborhoods would be considered. Similarly, as expressed in Section 2, more aggressive tubular neighborhoods may suffice for curves that are not C^2. It appears premature to pursue these enhancements for this application, as there will be additional local geometric information available indicating a

[12] The dissertation work [18] of the first author adopted an alternative, more explicit way to construct the ambient isotopy, with iteration of $\max\{N(\frac{\pi}{2n}), N'(r)\}$. It was shown [18, Remark 4.2.7] that $N(\frac{\pi}{2n}) < N\left(\frac{\pi}{2(n-1)}\right) + 1$, so that no more than 1 additional subdivision iteration would be used to produce the ambient isotopy after a homeomorphism is attained from Theorem 8.3. However, the method here has advantages because of its direct use of subdivision versus specialized techniques.

likely impending topological change which may lead to more direct and efficient options to zoom into that area for a purely local analysis.

The question of tightness[13] is a question of significant theoretical and practical interest. These authors see that investigation as beyond the scope of the present work, particularly as they conjecture that proving rigorous tightness bounds could be difficult. Support for that conjecture is based upon the subtlety of published constructions regarding topological properties of knotted splines [5, 19, 34].

10. Conclusion

We first proved the *exterior angles* of control polygons converge exponentially to zero under subdivision. We establish sufficient conditions for subdivision to produce a control polygon ambient isotopic to a Bézier curve, with *a priori* determination of a sufficient number of subdivision iterations. These results are being applied in computer animation, particularly for dynamic visualization of molecular simulations. The theorems given provide consistency and rigor to replace previously *ad hoc* animation techniques that were error prone by focusing only on one frame at a time. This examination is necessarily at a discrete point in time, whereas the analysis here is over the continuum of a time interval.

Acknowledgement: We very much appreciate the helpful, constructive comments of multiple referees. One of the reports was particularly comprehensive, well beyond typical expectations, for which we express additional thanks. Early discussions with Jorg Peters regarding the convergence of exterior angles to 0 under subdivision, are also acknowledged, with appreciation.

References

[1] N. Amenta, T. J. Peters, and A. C. Russell. Computational topology: Ambient isotopic approximation of 2-manifolds. *Theoretical Computer Science*, 305:3–15, 2003.

[13] This was constructively raised by one of the reviewers.

[2] L. E. Andersson, S. M. Dorney, T. J. Peters, and N. F. Stewart. Polyhedral perturbations that preserve topological form. *CAGD*, 12(8):785–799, 1995.

[3] L. E. Andersson, T. J. Peters, and N. F. Stewart. Selfintersection of composite curves and surfaces. *CAGD*, 15:507–527, 1998.

[4] L-E Andersson, T. J. Peters, and N. F. Stewart. Equivalence of topological form for curvilinear geometric objects. *International Journal of Computational Geometry & Applications*, 10(06):609–622, 2000.

[5] J. Bisceglio, T. J. Peters, J. A. Roulier, and C. H. Sequin. Unknots with highly knotted control polygons. *CAGD*, 28(3):212–214, 2011.

[6] M. Burr, S. W. Choi, B. Galehouse, and C. K. Yap. Complete subdivision algorithms, II: Isotopic meshing of singular algebraic curves. *Journal of Symbolic Computation*, 47:131–152, 2012.

[7] H. P. Cassidy, T. J. Peters, H. Ilies, and K. E. Jordan. Topological integrity for dynamic spline models during visualization of big data. In *Topological Methods in Data Analysis and Visualization III*, pages 167–183. Springer, 2014.

[8] F. Chazal and D. Cohen-Steiner. A condition for isotopic approximation. *Graphical Models*, 67(5):390–404, 2005.

[9] W. Cho, T. Maekawa, and N. M. Patrikalakis. Topologically reliable approximation in terms of homeomorphism of composite Bézier curves. *Computer Aided Geometric Design*, 13:497–520, 1996.

[10] E. Denne and J. M. Sullivan. Convergence and isotopy type for graphs of finite total curvature. In A. I. Bobenko, J. M. Sullivan, P. Schröder, and G. M. Ziegler, editors, *Discrete Differential Geometry*, pages 163–174. Birkhäuser Basel, 2008.

[11] M. P. do Carmo. *Differential Geometry of Curves and Surfaces*. Prentice Hall, Upper Saddle River, NJ, 1976.

[12] G. E. Farin. *Curves and Surfaces for Computer-Aided Geometric Design: A Practical Code*. Academic Press, Inc., 1996.

[13] K. E. Jordan, L. E. Miller, E. L. F. Moore, T. J. Peters, and A. Russell. Modeling time and topology for animation and visualization with examples on parametric geometry. *Theoretical Computer Science*, 405:41–49, 2008.

[14] K. E. Jordan, L. E. Miller, T. J. Peters, and A. C. Russell. Geometric topology and visualizing 1-manifolds. In V. Pascucci, X. Tricoche, H. Hagen, and J. Tierny, editors, *Topological Methods in Data Analysis and Visualization*, pages 1 – 13. Springer NY, 2011.

[15] J. M. Lane and R. F. Riesenfeld. A theoretical development for the computer generation and display of piecewise polynomial surfaces. *IEEE*, PAMI-2 NO.1, January 1980.

[16] D. Lasser. Calculating the self-intersections of Bézier curves. *Computers in Industry*, 12(3):259–268, 1989.

[17] J. Lasseter. Principles of traditional animation applied to 3d computer animation. *SIGGRAPH Comput. Graph.*, 21(4):35–44, 1987.

[18] J. Li. *Topological and Isotopic Equivalence with Applications to Visualization*. PhD thesis, University of Connecticut, U.S., 2013.

[19] J. Li, T. J. Peters, and K. E. Jordan. Knot visualization experiments for verifiable molecular movies. *Applied General Topology*, 2014, in press.

[20] J. Li, T. J. Peters, D. Marsh, and K. E. Jordan. Computational topology counterexamples with 3D visualization of Bézier curves. *Applied General Topology*, 2012.

[21] L. Lin and C. Yap. Adaptive isotopic approximation of nonsingular curves: the parameterizability and nonlocal isotopy approach. *Discrete & Computational Geometry*, 45 (4):760–795, 2011.

[22] T. Maekawa, N. M. Patrikalakis, T. Sakkalis, and G. Yu. Analysis and applications of pipe surfaces. *CAGD*, 15(5):437–458, 1998.

[23] L. E. Miller. *Discrepancy and Isotopy for Manifold Approximations*. PhD thesis, University of Connecticut, U.S., 2009.

[24] J. W. Milnor. On the total curvature of knots. *Annals of Mathematics*, 52:248–257, 1950.

[25] G. Monge. *Application de l'analyse à la géométrie*. Bachelier, Paris, 1850.

[26] E. L. F. Moore. *Computational Topology of Spline Curves for Geometric and Molecular Approximations*. PhD thesis, University of Connecticut, U.S., 2006.

[27] E. L. F. Moore, T. J. Peters, and J. A. Roulier. Preserving computational topology by subdivision of quadratic and cubic Bézier curves. *Computing*, 79(2-4):317–323, 2007.

[28] G. Morin and R. Goldman. On the smooth convergence of subdivision and degree elevation for Bézier curves. *CAGD*, 18:657–666, 2001.

[29] J. Munkres. *Topology*. Prentice Hall, 2nd edition, 1999.

[30] D. Nairn, J. Peters, and D. Lutterkort. Sharp, quantitative bounds on the distance between a polynomial piece and its Bézier control polygon. *CAGD*, 16:613–631, 1999.

[31] M. Neagu, E. Calcoen, and B. Lacolle. Bézier curves: topological convergence of the control polygon. *6th Int. Conf. on Mathematical Methods for Curves and Surfaces, Vanderbilt*, pages 347–354, 2000.

[32] N. M. Patrikalakis and T. Maekawa. *Shape Interrogation for Computer Aided Design and Manufacturing*. Springer, 2002.

[33] L. Piegl and W. Tiller. *The NURBS Book*. Springer, New York, 2nd edition, 1997.

[34] C. H. Sequin. Spline knots and their control polygons with differing knottedness. `http://www.eecs.berkeley.edu/Pubs/TechRpts/2009/EECS-2009-152.html`.

[35] M. Stone and T. D. DeRose. A geometric characterization of parametric cubic curves. *ACM Transactions on Graphics*, 8(3):147–163, 1989.